RSC Advances

PAPER

View Article Online
View Journal | View Issue

Check for updates

Cite this: *RSC Adv.*, 2025, **15**, 48363

Synergy of surfactants and hyperbranched PVAc copolymer emulsion enabling ecological sand fixation in high salt-affected sandy land

Wei Gong,[ab] Haonan Ji,[a] Siying Liu,[a] Shitong Xie,[a] Meilan Li*[ab] and Liangliang Chang[a]

To mitigate the impact of salt crystallization damage in highly saline sandy lands, this study first evaluated the salt tolerance of three surfactants (SDS, L23 and CTAB), their effects on NaCl crystallization behavior, and their influence on microbial growth in sandy soil. Surfactant L23 was subsequently selected for further investigation. Given the importance of its interactions, the adsorption characteristics of L23 on sand particle surfaces under varying salinity conditions were systematically examined. Additionally, changes in the properties and morphology of the emulsion after the addition of different amounts of L23 and 3% NaCl were analyzed. Finally, the sand-fixing performance of the L23-emulsion composite material, including compressive strength, wind erosion resistance, thermal aging stability, freeze–thaw stability, and water retention, was comprehensively evaluated. Field experiments were also conducted to assess its promoting effects on plant and microbial growth in saline deserts, so as to elucidate its ecological impact. The experimental results demonstrated that L23 effectively modulated the crystallization morphology of salt in sandy soil. When incorporated into the saline-tolerant P(VAc-DBM-AA-AM-IA-HBP) hyperbranched emulsion, L23 significantly enhanced its mechanical properties. Further studies confirmed that the L23-emulsion composite material markedly reduced the agglomeration damage caused by NaCl crystallization to sand-fixing materials, thereby improving sand fixation effectiveness. The composite also exhibited outstanding thermal aging resistance, freeze–thaw stability, and water retention capacity, enabling it to withstand temperature fluctuations in desert environments. The positive growth of plants and microorganisms observed in field experiments verified its reliable ecological benefits. This study provides a novel strategy for developing ecological sand-fixing materials aimed at combating desertification in saline desert areas.

Received 29th September 2025
Accepted 30th November 2025

DOI: 10.1039/d5ra07386c

rsc.li/rsc-advances

Open Access Article. Published on 08 December 2025. Downloaded on 2/15/2026 4:40:46 PM.
This article is licensed under a Creative Commons Attribution-NonCommercial 3.0 Unported Licence.

1 Introduction

The combined effects of marginal water irrigation and conventional agricultural practices are key drivers behind the acceleration of global soil degradation, which is manifested through widespread salinization, nutrient depletion, and desertification.[1–5] These interconnected processes pose a grave threat to global agricultural sustainability and socioeconomic stability.[6] Currently, more than 100 countries are affected by desertification on salt-affected soils, with nearly one billion hectares of degraded land concentrated mainly in the arid and semi-arid regions of Asia, Africa, Australia, and South America. In China, salt-affected soils cover an area of 99.13 million hectares that are undergoing desertification.[7] Saline desertification usually leads to a range of detrimental environmental impacts, including the triggering of dust storms, impairment of crop health, dispersion of contaminated sediments, leaching of fertilizers, and the accumulation of silt in irrigation channels.[8–10] Accordingly, the desertification process driven by soil salinization presents a significant threat to the viability of sustainable agriculture in moisture-deficient regions. Hence, widespread soil salinization, driven by intensive land use and wind erosion, has created a pressing need for systematic ecological restoration and sustainable management.[11]

To solve this problem, nations worldwide have been necessitated to devise viable measures for desertification reduction and prevention. Currently, the prevailing technologies for sand fixation broadly encompass mechanical, biological, chemical, and integrated comprehensive measures.[12–17] Conventionally, the reclamation of saline soils has primarily relied on the utilization of halophytic plants, such as *Sesuvium portulacastrum* L., *Clerodendron inerme Gaertn.*, *Suaeda maritima Dum.*, *Ipomoea pescaprae Sweet*, *Heliotropium curassavicum* L., and one tree species *Excoecaria agallocha* L.[18–24] Nevertheless, severe wind erosion in highly saline sandy soils adversely

[a]*Shangluo University/Key Laboratory of Comprehensive Utilization of Tailings Resources in Shaanxi Province, Shangluo, China*
[b]*Chengdu Institute of Organic Chemistry, Chinese Academy of Sciences, Chengdu, China*

© 2025 The Author(s). Published by the Royal Society of Chemistry

Open Access Article. Published on 08 December 2025. Downloaded on 2/15/2026 4:40:46 PM. This article is licensed under a Creative Commons Attribution-NonCommercial 3.0 Unported Licence.

impacts restoration efforts; consequently, using vegetation alone proved insufficient for achieving adequate seed germination. This study's findings underscore that stabilizing the sandy substrate is of paramount importance and must be addressed to successfully rehabilitate salt-degraded desert ecosystems.

Contemporary sand fixation strategies utilize a range of raw materials, including polymers, silicate minerals, and bio-based composites.[25–30] Of these, polymer materials have attracted particular prominence due to their efficacy as novel agents for mitigating sand-wind erosion. This category encompasses polyacrylamide, polyvinyl alcohol, vinyl acetate–ethylene copolymer emulsion, and polyurethane.[31–39] Field testing has been conducted for polyurethane (PU), a material developed by Japan's TORAY, in the saline sandy environments of Qinghai, China. Early data exhibited pronounced sand-fixing effects upon implementation. Nevertheless, progressive degradation of the material over time led to a rapid decline in its stabilization performance.[40] Additionally, the economic viability of PU is compromised by its substantial expense, limiting its potential for extensive utilization. Hence, the paramount considerations for materials used in the stabilization of high-salinity sandy lands are their efficacy and economic feasibility.

Usually, emulsion polymers, especially vinyl acetate-based varieties, typically provide substantial cost benefits without compromising adhesive performance.[41–44] Due to their distinctive properties, these emulsion-based materials have become a principal approach for addressing desertification.[45] However, the performance of polymeric sand-binding agents in saline environments depends not only on material properties, but also on sand surface topography and ambient environmental conditions. The presence of salt plays a particularly critical role throughout the sand stabilization process, thereby ultimately affecting the overall performance of the materials.[46] Initially, when applied to sand surfaces, the sand-fixing emulsion partially penetrates the substrate, with the majority of droplets remaining on the surface. At this stage, the aqueous phase of the emulsion dissolves NaCl deposits present in the sand matrix. Under natural conditions, the relatively low NaCl content in the sand-well below saturation concentration-causes the dissolved salt to migrate toward the surface *via* capillary action as water from the emulsion evaporates.[47] Once the saturation point is exceeded, continued evaporation induces NaCl crystallization and dispersion within the polymer film. Owing to the strong hygroscopic nature of NaCl, the embedded salt crystals undergo repeated cycles of moisture absorption, surface dissolution, and recrystallization during drying events. This cyclic process facilitates the formation of hardened NaCl aggregates. The development of these crystalline structures progressively disrupts the continuity of the polymer film, impairing its mechanical properties and ultimately reducing its effectiveness in sand fixation.

Surfactants, as amphiphilic compounds, have been extensively utilized in various environmental and engineering applications due to their ability to markedly alter interfacial tensions.[48,49] They are broadly categorized into anionic, cationic, nonionic, and amphoteric types, each possessing distinct characteristics and applicability. In the context of soil stabilization and dust control, previous studies have explored their potential. For instance, anionic surfactants like sodium dodecyl sulfate (SDS) have been investigated for soil wettability enhancement and crust formation for wind erosion control.[50,51] Similarly, nonionic surfactants, such as certain alkyl polyglucosides, are often favored in environmental applications for their generally lower toxicity and better compatibility with microorganisms.[52] Cationic surfactants have also been studied, albeit less frequently for this purpose, sometimes due to concerns regarding their biocidal effects.[53]

However, most prior research has focused on conventional soils or short-term performance. The application of surfactants for sand fixation under high-salinity conditions remains underexplored. The interplay between surfactant type, salt tolerance, microbial activity, and salt crystallization morphology is critical yet rarely addressed systematically. Therefore, in order to improve the sand-fixing capability of emulsion used in practical application for humidity areas, in the present work, we employed a salting-out crystallization strategy to systematically evaluate the effects of different surfactant types (anionic (SDS), cationic (CTAB), and nonionic (L23)) on NaCl crystal size distribution.[54] This screening methodology identified optimal surfactants for effectively controlling NaCl crystal morphology. This study aimed to investigate the efficacy of surfactants for sand fixation under high-salinity conditions, a domain that remains underexplored. We hypothesized that a nonionic surfactant (L23) would demonstrate superior performance due to its anticipated better salt tolerance and environmental compatibility compared to ionic surfactants (SDS, CTAB). Based on these findings, we further investigated the influence of surfactant concentration on key emulsion properties, particularly droplet size and zeta potential. Subsequently, emulsion, NaCl, and surfactant solutions were mixed at varying concentrations and solidified into films, enabling detailed analysis of their surface morphology and mechanical properties. Finally, by incorporating surfactants, we further assessed the sand-fixing performance of the emulsion applied to high-salinity sandy soil, with a focus on sand consolidation strength and water retention capacity. This study clarifies how the addition of surfactants affects the sand-fixing performance of the emulsion.

2 Experimental

2.1 Materials

P(VAc-DBM-AA-AM-IA-HBP) hyperbranched copolymerized emulsion was synthesized in our laboratory.[55] Nonionic surfactant, Pluronic L23 was supplied by Haian Petrochemical Corp. (Jiangsu, China), and was used as received. Anionic surfactant, sodium dodecyl sulfate (SDS) was purchased from Kelong Chemical Reagent Corporation (Chengdu, China) and was used without further purification. Analytical pure cetyltrimethylammonium bromide (CTAB) procured from Sinopharm Chemical Reagent co., Ltd (Beijing, China), and was used as received. Sodium Chloride (NaCl) procured from Guangdong Guanghua Sci-Tech Co., Ltd (Guangdong, China), was used for

 © 2025 The Author(s). Published by the Royal Society of Chemistry

Open Access Article. Published on 08 December 2025. Downloaded on 2/15/2026 4:40:46 PM. This article is licensed under a Creative Commons Attribution-NonCommercial 3.0 Unported Licence.

preparation of brine. Deionized water was used in all preparations.

2.2 Experimental procedures

2.2.1 Analysis of surfactants-induced salt tolerance. The surfactant's salt tolerance is a critical indicator for assessing the efficacy of sand-fixation treatments in high-salinity environments. We quantified the transmittance of middle-layer aqueous surfactant solutions across varying salinity levels using spectrophotometric measurements. A spectrophotometer (721, Shanghai XIPU instrument co., Ltd) was used to measure the transmittance of surfactants middle layer aqueous solution with different salinities at 318 K and 600 nm wavelength. The maximum salt tolerance of each surfactant was determined by a turbidity point measurement. Specifically, NaCl was gradually added to a surfactant solution, and the transmittance at 600 nm was monitored. The concentration at which a sharp decrease in transmittance occurred, indicating the onset of surfactant precipitation and a clear-to-turbid transition, was recorded as the maximum salt tolerance.[56] Additionally, the phase volume fraction diagram also offers an alternative approach for assessing surfactant salt tolerance. The pseudo-ternary phase diagram for the oil/water/surfactant system[57] was experimentally established at 318 K.

2.2.2 Effect of surfactants on microbial growth. Microorganisms significantly contribute to improving sand fertility and facilitating plant nutrition, simultaneously accelerating the conversion of sandy substrates into productive soil. Therefore, the proliferation of soil microorganisms represents a critical indicator for evaluating the efficacy of sand fixation measures. This study employed microbes isolated from sand samples obtained from the Golmud sandy region in Qinghai Province to assess the ecological impacts of surfactants SDS, CTAB, and L23. Sandy soil containing 3% NaCl was initially amended with SDS, CTAB and L23 at concentrations ranging from 1.0% to 5.0% (inclusive). After one month of storage at room temperature, the samples were immersed in distilled water to extract sand-associated microorganisms for subsequent analysis. The soil microbial population was quantified using adapted protocols based on the methods established by Mathur *et al.*[58] and Lima *et al.*[59] The data were examined by one-way analysis of variance (ANOVA) followed by Tukey-HSD tests using the SPSS statistical package. The level of significance was set at $p < 0.01$ or $p < 0.001$.

2.2.3 Effect of surfactants on NaCl crystallization. Owing to its remarkable salt tolerance and favorable ecological characteristics, L23 was chosen in this study to suppress and modify NaCl crystallization behavior, thus reducing its detrimental impacts. Specifically, NaCl was diluted to a concentration of 3.0 wt% using L23 aqueous solutions at different concentrations. Equal-volume specimens were subsequently prepared and dried at room temperature to promote crystallization.

The particle size distribution was measured by laser diffraction. Key parameters reported include: D_{50} (the median particle diameter), D_{90} (the diameter at the 90th percentile of the cumulative distribution), $D_{(4,3)}$ (the volume-weighted mean diameter, sensitive to the presence of larger particles), and $D_{(3,2)}$ (the surface-area weighted mean diameter, influenced by finer particles). The ratio of $D_{(4,3)}$ to $D_{(3,2)}$ serves as an indicator of the distribution breadth, with a higher value signifying a wider size distribution.

2.2.4 Adsorption behavior between L23 and salt-laden sand particles. A sequence of batch experiments was conducted to evaluate the influence of NaCl concentration on the adsorption capacity of sand particles for L23.[60] A total of 8.0 g of dried sand particles with varying salt contents (weighed to an accuracy of 0.001 g) was added to 250 mL conical flasks containing varying volumes of L23 solution, the initial concentration of L23 used in the adsorption studies was 2500 mg L^{-1}. The mixture was continuously agitated for 24 h at 303 K in a temperature-controlled horizontal shaker operating at 120 rpm to ensure complete adsorption. Then the L23 solutions were isolated with the treated sand particles by centrifugation. The equilibrium concentration (C_e) of L23 solutions were determined by the potassium ferrocyanide titration methods. The amount of L23 adsorbed on the adsorbent, Γ(mg g^{-1}), was calculated by a mass balance relation:

$$\Gamma = (C_0 - C_e)V/m$$

where, C_0 and C_e are the initial and equilibrium concentrations of L23 (mg g^{-1}) respectively, V is the volume of L23 solution (L), and m is the weight of the salt-laden sand particles (g) used.

2.2.5 Mechanical properties of films formed by L23 in salt-containing emulsion. A uniform mixture of P(VAc-DBM-AA-AM-IA-HBP) emulsion containing 3.0% NaCl and L23 solutions at different concentrations was poured into a polytetrafluoroethylene (PTFE) mold and dried under ambient conditions to form a film. The tensile strength and elongation at break of the films were measured using an LDW-20 electronic universal testing machine. The mechanical properties were determined by averaging measurements obtained from 5 samples in each replication.

2.3 Sand-fixing properties of L23 mixed with P(VAc-DBM-AA-AM-IA-HBP) emulsion

2.3.1 Preparation of fixed sand specimen. Based on the comprehensive evaluation of surfactant salt tolerance, effects on microbial growth, and NaCl crystallization behavior, only L23 was found to be suitable for practical application in sand fixation under high-salinity conditions. Therefore, in the sand fixation experiments, only L23 was used. Standardized specimens were prepared by homogeneously mixing 9.7 g of sand, 0.3 g of salt, and 1 g of 3.0% (w/w) emulsion with L23 at varying concentrations. The mixture was subsequently transferred into cylindrical molds (2.0 cm diameter × 2.2 cm height) to form consolidated sand columns for compressive strength testing. The specimens were first cured at ambient temperature for 4 h, followed by 15 days drying under identical conditions.

2.3.2 Compressive strength of fixed sand specimen. The compressive strength was measured using a universal testing machine (WDW-5; Jinan Chuanbai Instrument Co., Ltd China). The fully cured sand columns were tested under uniaxial

Open Access Article. Published on 08 December 2025. Downloaded on 2/15/2026 4:40:46 PM. This article is licensed under a Creative Commons Attribution-NonCommercial 3.0 Unported Licence.

compression at a constant displacement rate of 100 mm min^{-1} until structural failure occurred. The maximum stress observed during testing was recorded as the compressive strength (MPa), with triplicate measurements conducted for each sample group to ensure statistical reliability.

2.3.3 Water retention experiment. In the laboratory, a sand column model with a height of 35–45 mm and a diameter of 90 mm was prepared to evaluate the water retention performance of sand-fixing materials. The column was filled with a mixture of 97 g of sand and 3 g of salt. After a crust had formed on the surface following the application of various sand-fixing materials, water was sprayed onto the surface at a rate of 1 L m^{-2}. The moist specimens were then transferred to an oven and maintained at a constant temperature of 298 K. The water content of each salt-affected sand specimen was determined within 48 hours based on weight loss, with the reported value representing the average of three independent measurements:

$$\text{Water content} = [(\text{wet sand weight} - \text{dry sand weight})/\text{water weight}] \times 100\%$$

2.3.4 Anti-wind erosion experiment. A laboratory-assembled anti-wind erosion device was used to assess the wind erosion resistance of the sand columns. In preparation for the experiment, a mixture consisting of 97 g of sand, 3 g of salt, and 10 g of various sand-fixing materials was homogenized and then dried at ambient temperature for 21 days to simulate wind conditions of 16 m s^{-1} during the anti-wind erosion test. The weight of the sand-fixing system was recorded within 40 minutes, and the experiment was repeated three times.

2.3.5 Thermal aging ability of fixed sand specimen. To assess the durability under simulated desert conditions, which experience high diurnal temperature fluctuations, thermal aging was performed at 333 K for 24 days. These temperatures exceed the peak temperatures encountered in typical desert environments, thereby providing an accelerated assessment of the polymer's sand-fixing performance. The 24 days duration was chosen based on previous studies,[61] which demonstrated that it is sufficient to initiate and observe measurable changes in the mechanical properties of similar polymer-based sand-fixing agents. So, the specimen columns underwent heat aging in an air-circulation oven at 333 K for a total duration of 24 days, following a cyclic protocol. The compressive strength of each sample was measured after every cycle to assess the thermal aging stability of the sand-fixing material, and every cycle experiment was repeated three times.

2.3.6 Freezing–thawing resistance tests. Based on the climatic conditions typical of desert environments, freezing–thawing cycle tests were conducted over a temperature range of 253 K to 333 K. Freeze–thaw cycling was performed using an automated freeze–thaw testing apparatus (TL-010, Suzhou Zhihe Environmental Instrument Co., Ltd, Jiangsu, China). One complete freeze–thaw cycle consisted of 22 hours of freezing at 253 K followed by 2 hours of thawing at 333 K. The specimen column underwent 24 such cycles and was subsequently tested for compressive strength to evaluate the freeze–thaw stability of the sand-fixing material. The reported values represent the average of three replicate measurements.

2.4 Ecological effect of L23 mixed with P(VAc-DBM-AA-AM-IA-HBP) emulsion

2.4.1 Plants growth. To investigate the effect of sand-fixing composite materials on plant growth in sandy soil with a salt content of 3%, an outdoor cultivation experiment was conducted. Three treatment groups were established: CK (no material added), emulsion + 1% L23, and emulsion + 3% L23. After spraying ample water and allowing it to fully infiltrate the soil, a specific quantity of L23 treated the composite emulsion was applied at a rate of 1 L m^{-2}. A control group sprayed with an equivalent amount of water was set up for comparison. Plant growth was observed on the 60th day after transplanting two tomato seedlings into each pot. And then, a simulation ecological sand-fixing experiment was designed in saline sandy areas of Qinghai, that is, Tall Fescue, a kind of halophyte, was sowed in the salt-affected sand soil, and the emulsion + 3% L23 composite material was sprayed on the surface of the sand soil for sand fixation; hereafter, the growth of halophytes was observed.

2.4.2 Microorganism analysis. Six months later, triplicate soil samples were collected from a depth of 0–20 cm at each site using the salt-affected sandy soil to analyze microbial community changes. The microbial population in salt-affected sandy soils is typically quantified using the plate counting method.[62]

2.4.3 Effects of sand-fixing materials on sandy soil physicochemical properties. An outdoor experiment was carried out between March and September 2024 to evaluate the physicochemical properties of treated salt-affected sandy soils using the following methodologies: sand humidity was measured with a JXBS-3001-WRB-1 multi-parameter soil sensor (Weihai Jingxun Changtong Electronic Technology Co., Ltd, Shandong, China). Subsequently, at the same time each month, organic matter content was quantified by the potassium dichromate volumetric method, while total nitrogen content was determined using the standard Kjeldahl method[63] with an HN-01 Kjeldahl nitrogen analyzer (Shanghai Yonggui Analytical Instruments Co., Ltd, China). The analytical procedure comprised three principal steps: digestion in concentrated sulfuric acid with a catalytic mixture (K_2SO_4 and $CuSO_4$) at elevated temperature to convert organic nitrogen into ammonium sulfate; alkaline treatment of the digested sample followed by quantitative distillation of the liberated ammonia into boric acid absorption solution; and final titration of the captured ammonia with standardized hydrochloric acid. The total nitrogen content was calculated based on the titration data. Available phosphorus and potassium were measured using atomic emission spectrometry.

3 Results and discussion

3.1 Salt tolerance of surfactants

The salt tolerance of surfactants can be evaluated based on their water solubilization capacity at varying salinity levels.[64] As

 © 2025 The Author(s). Published by the Royal Society of Chemistry

Open Access Article. Published on 08 December 2025. Downloaded on 2/15/2026 4:40:46 PM.
This article is licensed under a Creative Commons Attribution-NonCommercial 3.0 Unported Licence.

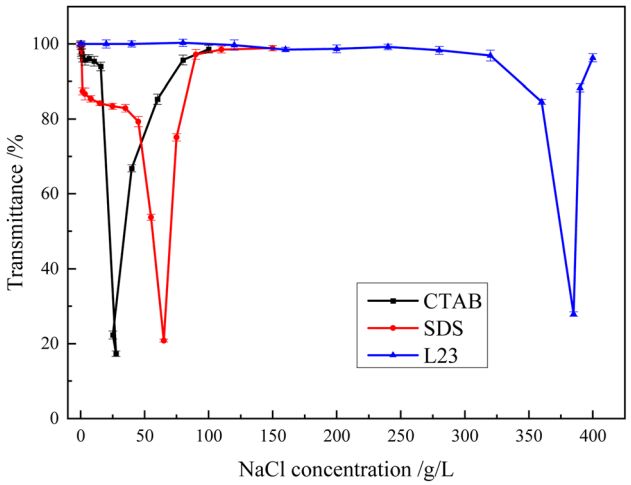

Fig. 1 Transmittance of the middle-phase surfactant aqueous solution as a function of electrolyte concentration at 318 K.

shown in Fig. 1, the transmittance of the middle aqueous phase in SDS, CTAB, and L23 solutions was measured across varying salt concentrations. The results demonstrate that as NaCl concentration gradually increases, a critical point is reached where the transmittance undergoes a sharp decrease, indicating the onset of phase separation within the system. The salt concentration corresponding to this sharp drop in transmittance is defined as the maximum salt tolerance for each surfactant.[65] Accordingly, the maximum salt tolerances were determined to be 27.6 g L^{-1} for CTAB, 65 g L^{-1} for SDS, and 385 g L^{-1} for L23. This critical transition signifies the collapse of micellar stability and the formation of surfactant aggregates, confirming that the surfactants maintain excellent salt tolerance below their respective threshold concentrations.

The distinct differences in salt tolerance can be attributed to the molecular structures of the surfactants. Both CTAB (cationic) and SDS (anionic) are ionic surfactants whose solubility heavily relies on electrostatic repulsion between charged headgroups. The addition of NaCl compresses the electrical double layer and screens these charges, effectively reducing intermolecular repulsion and leading to aggregation and precipitation at relatively low salt concentrations. In contrast, L23 is a non-ionic surfactant whose solubility derives from the hydration of its polyoxyethylene chain. This steric stabilization mechanism is significantly less affected by the presence of salt ions, thereby conferring its superior salt tolerance. Generally, the salt content in saline sandy soils is below 3%. These results indicate that both SDS and L23 are suitable for sand fixation in highly saline sandy land environments.

The salinity at which surfactant water solubilization reaches its maximum is generally defined as the "optimal salinity" for microemulsion systems.[66] Typically, this optimal salinity occurs within the Winsor III region, where the solubilization parameters of oil and water (σ_o and σ_w) in the microemulsion phase are equal, corresponding to the minimum interfacial tension.[67] Based on the experimental results shown in Fig. 2, the optimal salinities of SDS and L23, as determined through phase behavior analysis, were identified as 60 g L^{-1} and 100 g L^{-1}, respectively (Table 1). Furthermore, it was observed that at the optimal salinity, the middle-phase microemulsion exhibited the capability to solubilize equal volumes of oil and brine. Therefore, it can be stated with high confidence that the composite sand-fixing material prepared with SDS and L23 remains stable at the optimal salinity, even under conditions far exceeding the actual salt content typically found in sandy lands.

Besides, the salt tolerance of surfactants can be evaluated based on the salinity range (denoted as $\Delta S = S_2 - S_1$, where S_1 represents the initial salinity and S_2 corresponds to the final salinity at which the middle-phase microemulsion forms). Because the salt content in the saline sandy land was generally below 3%, which is significantly lower than the ΔS values of both SDS and L23, it can be concluded that SDS and L23 are suitable for use in sand-fixing materials applied to highly saline-affected sandy lands (Table 1).

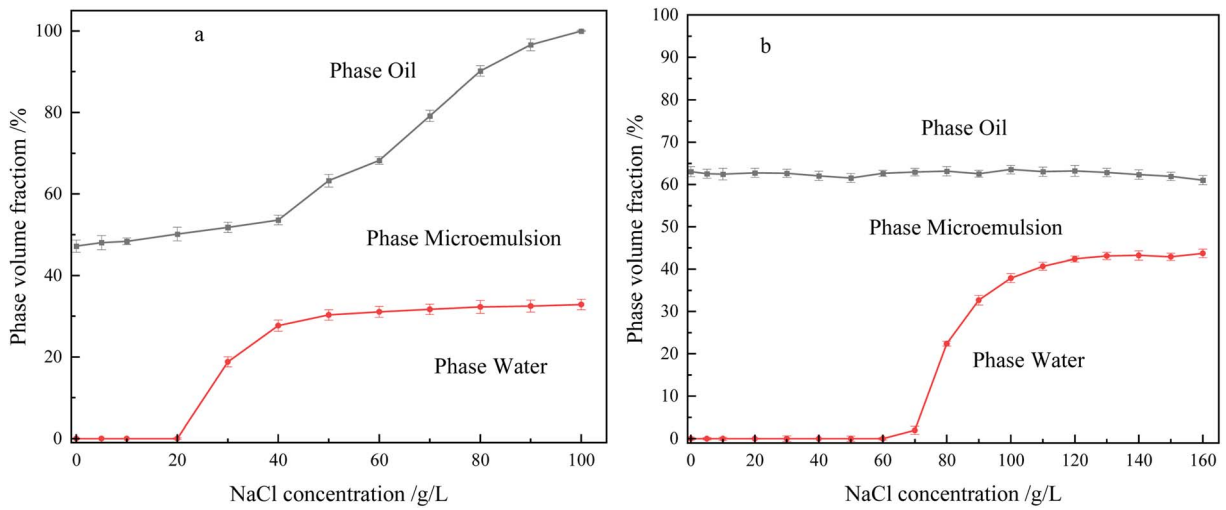

Fig. 2 Phase volume fractions of the oil, microemulsion, and aqueous phases as a function of NaCl concentration at 318 K: (a) SDS, (b) L23.

Open Access Article. Published on 08 December 2025. Downloaded on 2/15/2026 4:40:46 PM. This article is licensed under a Creative Commons Attribution-NonCommercial 3.0 Unported Licence.

Table 1 Optimal salinity (S^*), initial salinity (S_1), end salinity (S_2), and salinity range ($\Delta S = S_2 - S_1$) for obtaining middle phase emulsion with SDS or L35 at 318 K[a]

	S^* (g L^{-1})	S_1 (g L^{-1})	S_2 (g L^{-1})	ΔS (g L^{-1})
SDS	60	30	90	60
L23	100	70	>160	>90

[a] The volume fractions of the three macroscopic phases are normalized to 100%. The co-surfactant (*sec*-butyl alcohol) is solubilized within the microemulsion phase and is not represented as an independent component.

3.2 Ecological effect of the surfactant on high salt-affected sandy land

Microorganisms contribute substantially to sandy soil fertility and plant nutrition, while also promoting the conversion of sand into soil. Moreover, they are recognized as the most biologically dynamic constituents in terrestrial ecosystems. As a result, microbial growth and activity represent a key indicator for assessing the efficacy of sandy land restoration efforts. Due to CTAB exhibits significant inhibitory effects on soil microbial growth. Since a sustainable sand-fixation strategy should promote or at least not harm the soil ecosystem, the bactericidal properties of cationic surfactants like CTAB make them an undesirable choice. Therefore, Table 2 showed the bacterial counts in sand treated with 3.0% salt along with varying concentrations of SDS and L23. As observed, increasing the concentration of L23 did not significantly affect the bacterial population in the sand. Although SDS was able to inhibit bacterial growth to some extent, a substantial number of sand bacteria remained present in the culture. These results indicated that, at the tested concentrations, both SDS and L23 were harmless to the growth of sandy soil microorganisms. Moreover, the composite sand-fixing material prepared with SDS and L23 not only exhibited excellent salt tolerance, but also demonstrated positive ecological effects when applied in highly saline sandy land.

3.3 Effects of surfactants on the crystallization behavior of NaCl

To reduce the influence of NaCl crystal size on sand fixation efficiency, multiple types of surfactants were incorporated during the crystallization of NaCl to investigate their effects on its crystallization behavior. As shown in Fig. 3, in the absence of surfactants, the strong hygroscopicity of NaCl induced dissolution and recrystallization on the crystal surfaces. This process promoted the formation of crystalline bridges at interparticle contact points, which caused particle adhesion and ultimately led to the development of large aggregates (Fig. 3(a)). Upon addition of SDS or CTAB to the NaCl solution, precipitation of the surfactants occurred during crystallization as the NaCl concentration exceeded their respective salt tolerance limits. This loss of surfactant activity due to precipitation consequently eliminated their ability to modify the surfaces of NaCl crystals (Fig. 3(b) and (c)), which demonstrate that SDS and CTAB lacked adequate salt tolerance and failed to prevent the formation of

Table 2 The change in soil bacterial quantity of sand specimens treated with different concentrations of surfactant after 30 days[a]

The surfactant concentration (%)	Bacteria (/g) of spraying SDS	Bacteria (/g) of spraying L23
0	$(2.017 \pm 0.0416) \times 10^{5a}$	$(2.084 \pm 0.0279) \times 10^{5a}$
1	$(2.035 \pm 0.0761) \times 10^{5a}$	$(2.053 \pm 0.0162) \times 10^{5a}$
2	$(1.919 \pm 0.0549) \times 10^{5a}$	$(2.048 \pm 0.0613) \times 10^{5a}$
3	$(1.874 \pm 0.0431) \times 10^{5a}$	$(2.091 \pm 0.0157) \times 10^{5a}$
4	$(1.736 \pm 0.0904) \times 10^{5b}$	$(2.027 \pm 0.0285) \times 10^{5b}$
5	$(1.419 \pm 0.0746) \times 10^{5a}$	$(2.044 \pm 0.0386) \times 10^{5a}$

[a] Level of significance: $p < 0.001$ between sand specimens treated with different concentrations of surfactant according to Student's *t*-test. [b] Level of significance: $p < 0.01$ between sand specimens treated with different concentrations of surfactant according to student's *t*-test. Data for CTAB is not presented due to its severe biocidal effect, which resulted in complete inhibition of microbial activity and precluded meaningful quantitative comparison. This property is a key factor in its unsuitability for ecological applications.

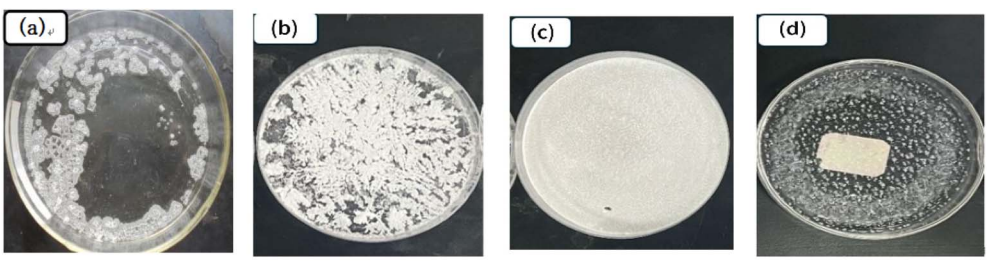

Fig. 3 Effects of different surfactants on the crystallization behavior of NaCl: (a) CK; (b) 3% CATB; (c) 3% SDS; (d) 3% L23.

© 2025 The Author(s). Published by the Royal Society of Chemistry

Open Access Article. Published on 08 December 2025. Downloaded on 2/15/2026 4:40:46 PM. This article is licensed under a Creative Commons Attribution-NonCommercial 3.0 Unported Licence.

large, destructive salt crystals within the sand matrix. In contrast, owing to its exceptional salt tolerance, the introduction of L23 into the NaCl solution markedly suppressed moisture absorption and prevented the caking of NaCl crystals. Consequently, L23 facilitated the formation of smaller NaCl crystals (Fig. 3(d)). The underlying mechanism originated from the active participation of L23 in the crystal growth process without integration into the crystal lattice. Instead, it accumulated near or adsorbed directly onto crystal surfaces. Shortly after nucleation, L23 rapidly adsorbed at the solid–liquid interface, forming a molecular film that functions as an effective anti-caking barrier. This film not only reduced moisture uptake by NaCl, thereby decreasing crystal water content, but also promoted dehydration. Moreover, L23 molecules adopt a zigzag conformation in aqueous solution, with hydrocarbon chains constituting a hydrophobic domain on one side and polyether oxygen groups forming a hydrophilic domain on the opposite side. Upon adsorption, L23 oriented its polar groups toward the crystal interior while positioning nonpolar groups outward, creating a thin hydrophobic encapsulation layer around the crystal. This layer effectively obstructed atmospheric moisture absorption by NaCl, thus inhibiting water adsorption and suppressing dissolution and recrystallization on the crystal surface.[68] As a result, it significantly reduced or entirely eliminated the caking tendency of NaCl. Furthermore, the hydrophobic film served as a mechanical barrier between adjacent crystals, further preventing intergranular agglomeration and leading to a decrease in NaCl crystal size, which is crucial for maintaining the structural integrity of the sand-fixing layer.

3.4 XRD analysis

X-ray diffraction (XRD) analysis was conducted on NaCl particles after L23 surface modification and subsequent heat treatment at 673 K to remove the modifier. Phase identification was carried out by comparing the obtained diffraction patterns with standard powder diffraction data from the International Centre for Diffraction Data (ICDD) database, specifically referencing the JCPDS card No. 01-077-2064 for NaCl. As shown in Fig. 4, all diffraction peaks of the modified powder precisely matched the standard peak positions of pure NaCl, confirming that the crystal structure, particularly its cubic characteristics, remained intact throughout the entire process of L23 modification and subsequent removal. In other words, the L23-modified powder retained the crystalline phase of sodium chloride, demonstrating that the modification process did not alter the NaCl crystal structure. These results further verified that surfactants played an essential role in regulating the morphology and size of NaCl particles during crystal growth. Specifically, surfactant adsorption on crystal surfaces lowered the interfacial energy required for nucleation, thereby enhancing the nucleation rate. On the other hand, surfactants also inhibited secondary nucleation by blocking key sites on crystal facets, reducing NaCl collision probability, and occupying active nucleation centers. Additionally, the encapsulation layer formed by surfactants around the crystal nuclei disrupted hydrogen-bond bridging between water molecules and NaCl crystals, effectively preventing particle agglomeration.[69] Our results strongly support the initial hypothesis, demonstrating that L23 was the only surfactant suitable for high-salinity sand fixation. This confirms the critical importance of selecting nonionic surfactants for saline environment restoration, a nuance that was previously suggested but not conclusively demonstrated.

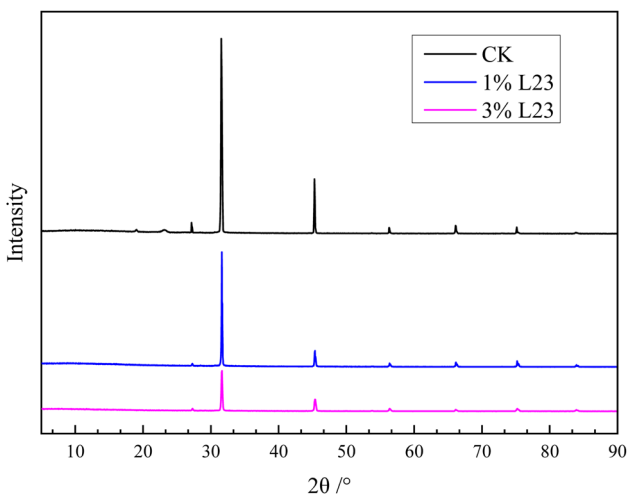

Fig. 4 The XRD of NaCl particles with different dosages of L23.

The beneficial effects of L23 on NaCl particle size and dispersion were confirmed by the particle size analysis results in Table 3. This study employed the volume-weighted mean diameter $D_{(4,3)}$ (De Brouckere mean, sensitive to the presence of larger particles) and the surface-area weighted mean diameter $D_{(3,2)}$ (Sauter mean diameter, more influenced by finer particles) as characterization metrics. Data analysis demonstrated a clear inverse correlation between L23 concentration and the width of particle size distribution.

This regularity indicates that L23 effectively regulates the NaCl crystallization process by suppressing excessive crystal growth and aggregation, thereby significantly reducing the hygroscopicity, deliquescence, and caking tendency of the resulting product. Consequently, the damaging effects of NaCl aggregates on sand-fixing materials are effectively suppressed, leading to significantly enhanced stability of sand fixation effectiveness.

3.5 Effect of salt concentration on adsorption isotherm of L23

The investigation into how NaCl concentration affects L23 adsorption on sand particles is essential, given that the sand-fixing material is designed for highly saline environments.

Table 3 Size distribution of NaCl particles with different L23 content

L23 dosage/%	D_{50}/μm	D_{90}/μm	$D_{(4,3)}$/μm	$D_{(3,2)}$/μm	$D_{(4,3)}/D_{(3,2)}$
0	29.14	54.71	22.27	4.06	5.49
1	19.05	33.75	17.25	3.81	4.53
3	7.49	11.79	8.05	3.61	2.23

Open Access Article. Published on 08 December 2025. Downloaded on 2/15/2026 4:40:46 PM.
This article is licensed under a Creative Commons Attribution-NonCommercial 3.0 Unported Licence.

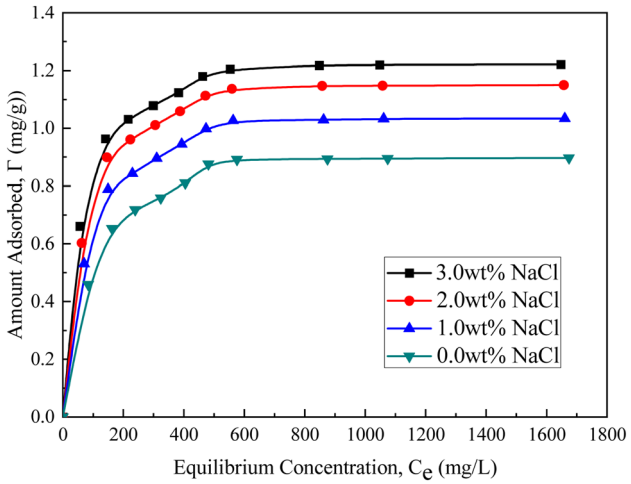

Fig. 5 Adsorption isotherms of L23 on sand surface at varied salinities of brine at 303 K.

Adsorption isotherms for L23 solution at varied salinities were shown in Fig. 5, the adsorption capacity of L23 on sand particles exhibited a progressive increase with higher NaCl concentrations before eventually plateauing. This phenomenon can be primarily attributed to the following mechanisms, firstly, Na^+ and Cl^- ions compressed the diffuse double layers of both the sand surface and L23 molecules, effectively reducing electrostatic repulsion and strengthening the van der Waals forces and hydrophobic interactions between the hydrophobic chains of L23 and the sand particles; secondly, the "salting-out effect" induced by salt ions decreased the solubility of L23 in the solution, driving its migration from the liquid phase to the solid–liquid interface. Meanwhile, Na^+ ions reduced the negative surface potential of the sand through charge neutralization, lowering the adsorption energy barrier for the polar head groups of L23. These synergistic effects collectively optimized the thermodynamic and kinetic processes of L23 adsorption at the sand interface,[70,71] thereby improving its adsorption efficiency. The finding told that the adsorption of L23 on sand particle was favored at high salinity and therefore, the adsorption process was found to be a chemical process with increasing salinity.

To gain a comprehensive understanding of the adsorption mechanism, the adsorption data were analyzed using both Langmuir and Freundlich isotherm models. These models were employed complementarily to evaluate the nature of the adsorption process and the heterogeneity of the sand surface. The Langmuir model, which presupposes monolayer adsorption onto a homogeneous surface with sites of uniform energy, was primarily used to estimate the maximum adsorption capacity (Q_m), thereby enabling a quantitative comparison of surfactant performance.[72] In contrast, to account for potential adsorption on heterogeneous surfaces, the Freundlich model was also applied. The Freundlich model, an empirical equation adept at describing adsorption on heterogeneous surfaces, was applied as a comparative benchmark. The parameters obtained from the two adsorption models are summarized in Fig. 6 and Table 4. Despite the complex nature of soil–surfactant interactions potentially deviating from the model's ideal assumptions, the regression coefficients (R^2) for the Langmuir model were consistently higher than those for the Freundlich model, the Langmuir equation still yielded a satisfactory empirical fit to the equilibrium data ($R^2 > 0.979$), indicating that the Langmuir isotherm described the adsorption behavior of L23 onto sand particles more accurately.

3.6 Effects of L23 on the properties of salt-containing emulsions

3.6.1 Particle size and zeta potential. The performance of sand-fixing emulsions on sandy surfaces is largely determined by their particle size and zeta potential, owing to the micropores and negative surface charges of sand particles. This study examined how the dosage of L23 influenced these two key

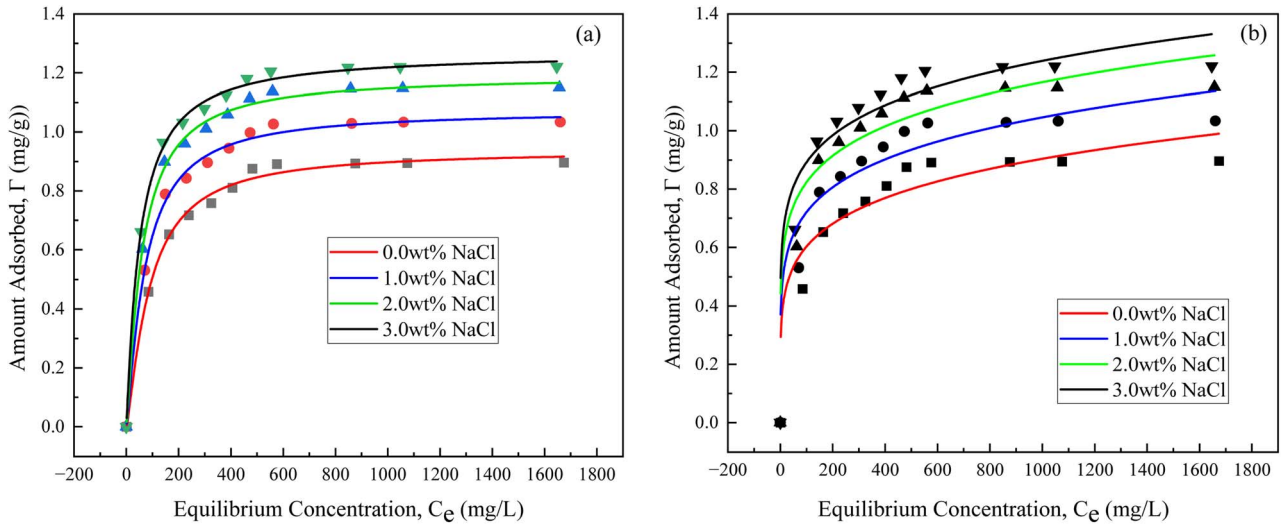

Fig. 6 Fitting curves of the adsorption of L23 on sand surface at varied salinities: (a) Langmuir; (b) Freundlich.

© 2025 The Author(s). Published by the Royal Society of Chemistry

Open Access Article. Published on 08 December 2025. Downloaded on 2/15/2026 4:40:46 PM. This article is licensed under a Creative Commons Attribution-NonCommercial 3.0 Unported Licence.

Table 4 Adsorption isotherm parameters of L23 at varied salinities

	Langmuir parameters			Freundlich parameters		
Salinities (wt% NaCl)	Γ_{max}(mg g^{-1})	$K_L \times 10^2$(L mg^{-1})	R^2	K_F(mg g^{-1})	$1/n$	R^2
0	0.937	0.328	0.979	0.268	0.176	0.791
1	1.072	0.538	0.984	0.342	0.162	0.793
2	1.189	0.777	0.988	0.411	0.151	0.793
3	1.267	1.385	0.990	0.462	0.143	0.808

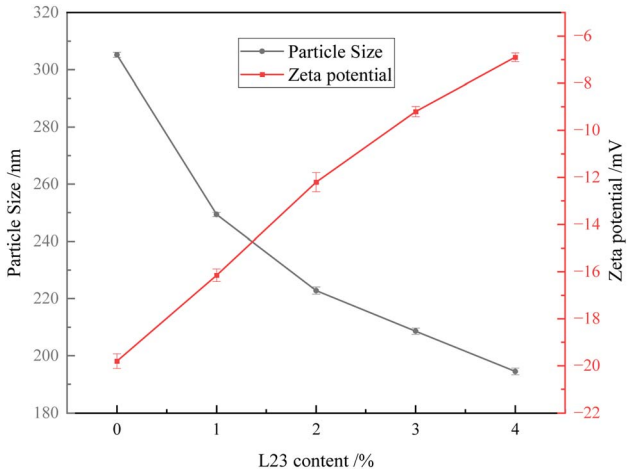

Fig. 7 The influence of L23 content on the particle size and zeta potential of the P(VAc-DBM-AA-AM-IA-HBP) emulsion containing 3.0% NaCl.

parameters. As illustrated in Fig. 7, increasing the L23 concentration effectively controlled the particle size of the saline emulsion through reinforcement of the surfactant adsorption layer, improved resistance to salt ion interference, and optimization of the micelle structure. The mechanism could be interpreted as follows: in NaCl-containing emulsion systems, inorganic salts could displace emulsifiers originally adsorbed on polymer chains. The interaction between emulsifiers and salt ions caused desorption and marked compression of the electric double layer, leading to a significant increase in apparent emulsion particle size. In contrast, when L23 was introduced, salt ions preferentially interact with L23, which strengthened the oil–water interfacial film and consequently reduced emulsion particle size.

As for the zeta potential, since L23 was a non-ionic surfactant, increasing its concentration lowered the negative charge density of the emulsion. This reduction in zeta potential electronegativity produced dual effects: on one hand, it diminished the coulombic repulsion between emulsion droplets and sand particles, and the improved electrostatic compatibility enhanced the adsorption of the saline emulsion onto the sand surface; on the other hand, the relatively low zeta potential values of particles in the system indicated limited colloidal stability, predisposing the system to demulsification and particle aggregation. While this represents a disadvantage for applications requiring long-term dispersion stability, it proves to be a crucial advantage for sand fixation. The tendency for rapid aggregation upon contact with the sand layer, coupled with water evaporation, constitutes the fundamental mechanism facilitating the formation of a dense, consolidated crust. This crust effectively binds sand particles together, thereby fulfilling the core functional requirement of wind erosion control. Consequently, the zeta potential characteristics observed in this study do not indicate performance flaws but are inherently linked to the system's designed functionality for rapid crust formation and efficient sand fixation.

3.6.2 SEM analysis. To understand how L23 enhanced the film-forming properties of saline emulsions, we examined the morphology of films derived from L23-modified emulsions (Fig. 8). In the absence of L23, the film contained large aggregates of NaCl particles embedded in the polymer matrix, along with numerous voids and significant interfacial debonding (Fig. 8(a)). A clear boundary with multiple interfacial cavities was observed between the NaCl particles and the polymer, indicating a thin transition layer and poor adhesion, which resulted in low interfacial bonding strength. As the L23 content increased, the NaCl crystal size decreased effectively, eliminating large visible particles on the film surface. Particle

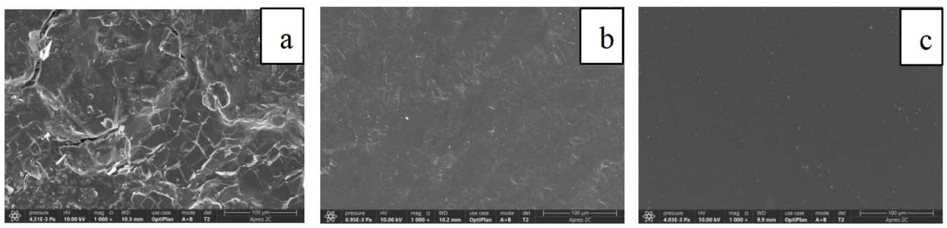

Fig. 8 Effect of L23 addition on the microscopic morphology of films formed from salt-containing emulsions: (a) CK; (b) 1% L23; (c) 3% L23.

Open Access Article. Published on 08 December 2025. Downloaded on 2/15/2026 4:40:46 PM. This article is licensed under a Creative Commons Attribution-NonCommercial 3.0 Unported Licence.

dispersion improved significantly, yielding a finer and more compact film structure. At 3% L23, the NaCl particles were completely incorporated into the composite matrix, leading to a highly blurred interface (Fig. 8(c)). The enhanced mechanical and functional properties of the film were attributed to the L23-induced refinement of NaCl particles and the formation of a high-strength interfacial transition zone. This particle-polymer synergy improved sand particle encapsulation and adhesion, leading to superior performance of the emulsion in high-salinity sand stabilization applications.

3.6.3 Mechanical properties. Similarly, the influence of L23 dosage on the mechanical properties of films derived from salt-containing emulsions was examined. As shown in Fig. 9, the tensile strength of the composite films first increased and then decreased with higher L23 content, peaking at 3.57 MPa for the film with 3% L23. This trend was attributed to the dual role of L23: it reduced NaCl particle size while plasticizing the surrounding polymer chains, thereby strengthening the interface. This enhanced interfacial interaction promoted shear-induced deformation under tension, initially improving tensile strength. Beyond an optimal dosage, however, the dominant external plasticizing effect led to a gradual strength reduction. In contrast, the elongation at break increased steadily with L23 content, due to the combined effected of finer particles, increased chain mobility, and external plasticization.[73]

3.7 Effect of L23 addition on sand fixation performance

3.7.1 Compressive strength. Compressive strength, indicating the mechanical resistance and interparticle bonding of the sand-fixing crust, was measured using naturally saline sand (≈3% salt) from mobile dunes in the Qinghai Sandy Land. The specimens were fabricated by mixing the sand with the emulsion and L23 with concentrations ranging from 0.0% to 4.0% according to the procedure described in Section 2.3.1. Fig. 10 showed that the compressive strength of the fixed sand exhibited a positive correlation with L23 concentration. The

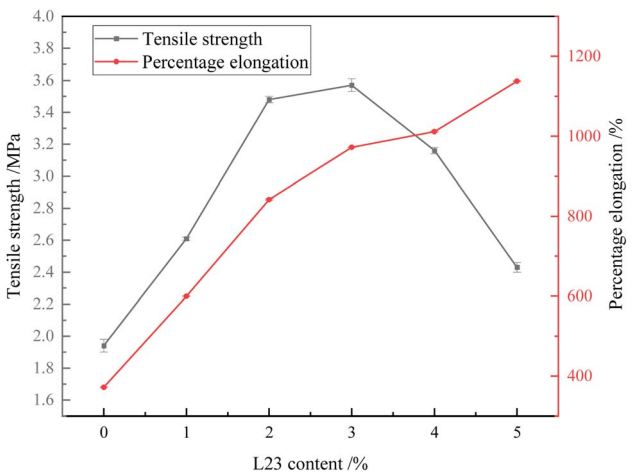

Fig. 9 Effect of L23 on the mechanical properties of salt-containing emulsions.

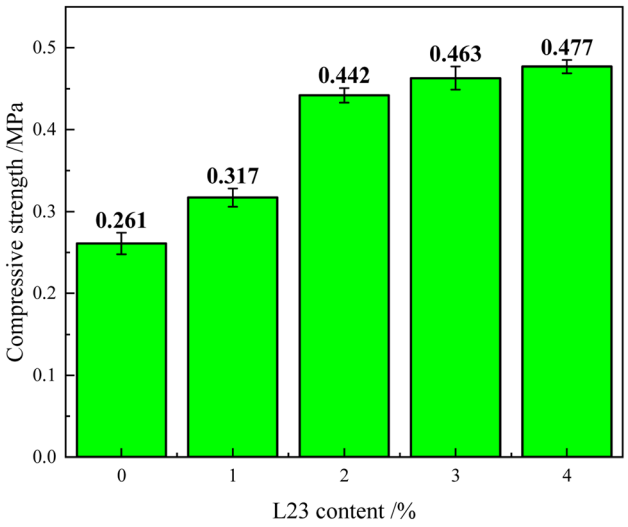

Fig. 10 Variation of compressive strength with L23 content in the emulsion.

sand-fixing strength of the sand mold exhibited a gradual increase with higher L23 addition. Upon reaching a 2% L23 dosage, the strength stabilized, showing only negligible subsequent variation. This behavior was attributed to the fact that, in the absence of L23, NaCl crystallized freely within the sand mold. The salt's strong hygroscopicity led to repeated dissolution–recrystallization cycles on the mold surface, which consequently promoted the growth of NaCl particles (Fig. 11(a)). As a result, the material's sand-fixing capability was significantly compromised. However, as the L23 content increased, it acted to both reduce the size of NaCl particles and form a hydrophobic protective layer around them, which in turn suppressed moisture absorption and particle agglomeration. Consequently, the detrimental effect of NaCl on the film was mitigated, leading to a progressive improvement in sand-fixing efficiency (Fig. 11(b)). However, when the L23 content exceeded 2%, its function shifted predominantly to that of an external plasticizer. The combined action of plasticization and particle stabilization resulted in a plateau in sand-fixing strength. These findings collectively demonstrated that the combined use of L23 and the P(VAc-DBM-AA-AM-IA-HBP) emulsion constituted a highly suitable composite sand-fixing material system for applications in high-salinity sandy environments.

3.7.2 SEM analysis. High-salinity conditions readily promote the formation of cracks and pores in latex films, adversely affecting their mechanical integrity and sand-fixing capacity. As shown in the SEM images, the surface of the salt-containing latex film without L23 was relatively rough and exhibited noticeable cracking and damage (Fig. 12(a)), mainly resulting from salt hygroscopicity and stress-induced damage during crystal growth within the film. In contrast, films modified with L23 displayed a notably smoother and denser surface morphology, with substantially fewer cracks and pores (Fig. 12(c)). To more precisely identify the distribution of crystalline structures in the sand sample shown in Fig. 12(c), EDS elemental mapping was performed on the annotated region of

© 2025 The Author(s). Published by the Royal Society of Chemistry

Open Access Article. Published on 08 December 2025. Downloaded on 2/15/2026 4:40:46 PM. This article is licensed under a Creative Commons Attribution-NonCommercial 3.0 Unported Licence.

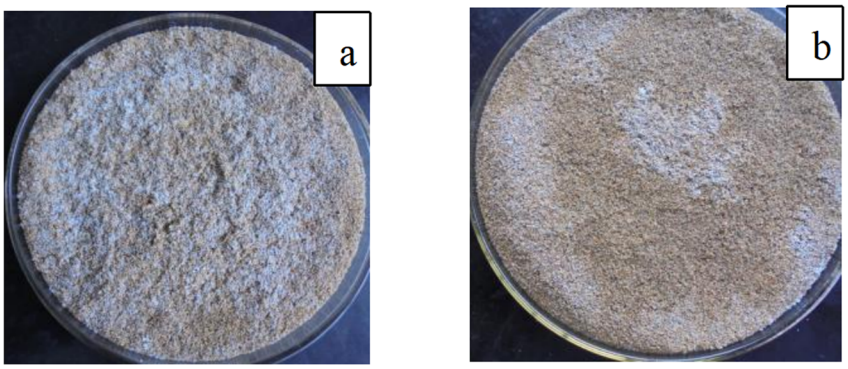

Fig. 11 Solidification effect on saline sand by L23 concentration in the emulsion: (a) CK; (b) 1% L23.

Fig. 12(c). The distribution maps for sodium and chlorine (Fig. 12(d) and (e)) demonstrate significant spatial co-localization of these two elements within the pores of the sand matrix, forming distinct aggregates. These results provide direct confirmation that the crystals are indeed NaCl, thereby verifying our research hypothesis that in the presence of L23, the salt crystallization process occurs in a dispersed manner rather than forming large, destructive crystalline crusts. These observations further verified that L23 incorporation effectively reduced the disruptive effects of NaCl particles on the film, significantly strengthened the mechanical performance of salt-containing latex films, and improved their durability against external physical stresses such as wind and rain erosion, leading to enhanced sand-fixing performance.

3.7.3 Anti-wind erosion performance. Fig. 13 presented the results of wind erosion resistance tests conducted through physical simulations using natural wind exposure on sand pile models. Under a wind speed of 16 m s^{-1}, compared to the control group's residual sand mass of 1.92%, the combined use of the emulsion and L23 increased the residual sand mass to 69.6%, meeting the wind erosion resistance standards for high-salinity sandy environments.[74] This phenomenon could be attributed to the addition of L23, which further reduced the particle size of NaCl, resulting in sufficiently fine NaCl particles with excellent compatibility with the polymer film. Under these conditions, the rigid NaCl particles effectively enhanced the polymer properties, thereby improving the sand-fixing performance of the P(VAc-DBM-AA-AM-IA-HBP) emulsion. Notably, the hyperbranched structure in the emulsion also reduced the interfacial tension between sand particles and the emulsion, consequently improving wettability and interfacial bonding strength.[75,76] So, adding L23 into P(VAc-DBM-AA-AM-IA-HBP) emulsion would be a prospective method for the ecological sand-fixation in high salt affected sandy land areas.

3.7.4 Thermal aging ability. To evaluate the thermal stability of the emulsion + L23 composite for sand fixation, saline sand containing 3% NaCl was treated with different sand-fixing materials and subjected to continuous thermal aging tests. As shown in Fig. 14, compressive strength remained largely unchanged over 24 thermal cycles, demonstrating

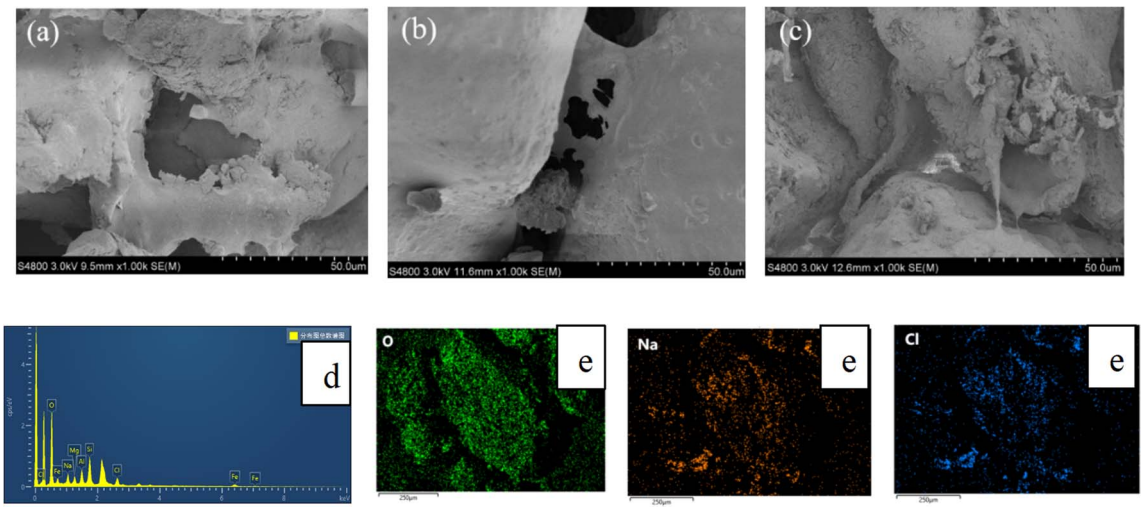

Fig. 12 Effect of L23 addition on the microscopic morphology of the emulsion in high-salinity sandy soil: (a) CK; (b) 1% L23; (c) 2% L23; (d) EDS spectra of (c) sample; (e) EDS mapping of (c) sample.

Open Access Article. Published on 08 December 2025. Downloaded on 2/15/2026 4:40:46 PM.
This article is licensed under a Creative Commons Attribution-NonCommercial 3.0 Unported Licence.

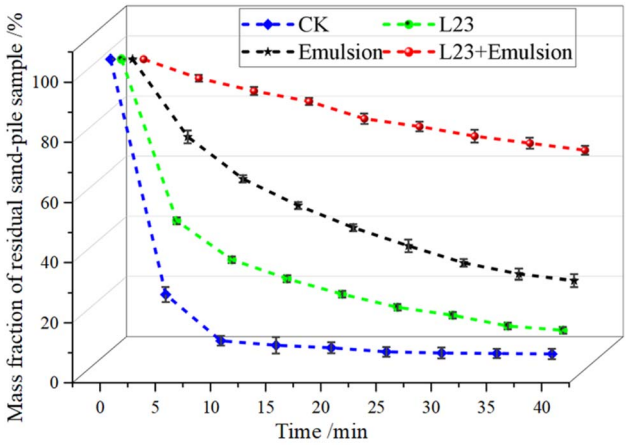

Fig. 13 Anti-wind erosion performance of the sand-pile models.

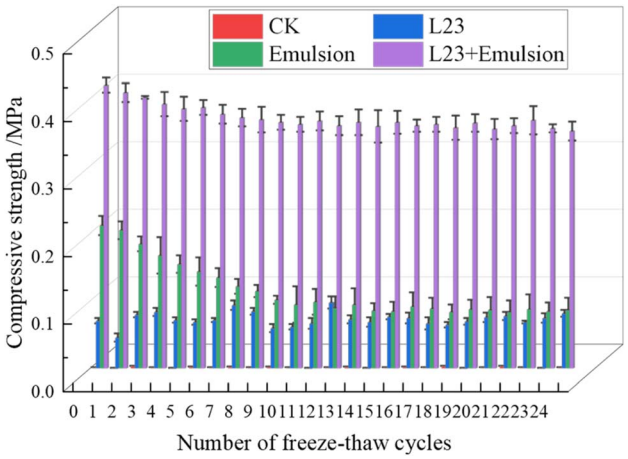

Fig. 15 Variation characteristics in compressive strength of freeze–thaw cycle frequency.

consistent performance regardless of the number of aging cycles. This observation demonstrates the robust thermal aging resistance inherent in the combined use of the emulsion and L23 consolidated sand layers.

3.7.5 Freeze–thaw ability. The freeze–thaw durability of sand layers consolidated with the emulsion + L23 composite was assessed. Specimens were prepared by treating sand (containing 3% NaCl) with different sand-fixing materials and subsequently tested for compressive strength. As illustrated in Fig. 15, a progressive decline in compressive strength was observed across all specimens as the number of freeze–thaw cycles increased. Notwithstanding this trend, the compressive strength retained after 24 cycles was 0.351 MPa, fulfilling the requisite standard. It can be concluded that the combined application of emulsion and L23 confered commendable frost resistance, indicating its suitability for sand stabilization in saline desert conditions.

3.7.6 Water retention performance. In order to increase available water capacity and promote the growth of halophytic vegetation, the water content of each specimen treated with different sand-fixing materials during different drying time was determined to evaluate the water-retaining ability. The relation curves of the water content of each specimen and drying time were presented in Fig. 16. It could be seen that the water content of treated specimens was much higher than that of untreated specimens during the test period. When no L23 was added to the emulsion, the large NaCl particles formed in the sand caused significant damage to the sand-fixing material, leading to the formation of channels with varying pore sizes between the film and sand particles. This allowed water molecules to move freely through these pathways, reducing resistance to evaporation and consequently decreasing the water retention capacity of the emulsion. However, with the addition of L23 to the emulsion, the size of NaCl crystals was effectively controlled and reduced, while phase separation between NaCl and the film was also minimized. Furthermore, the hydrophilic ends of L23 interacted with both free and bound water in the sand, forming a reticular molecular film that restricted the diffusion of water molecules into the air.[77] As a result, the water retention

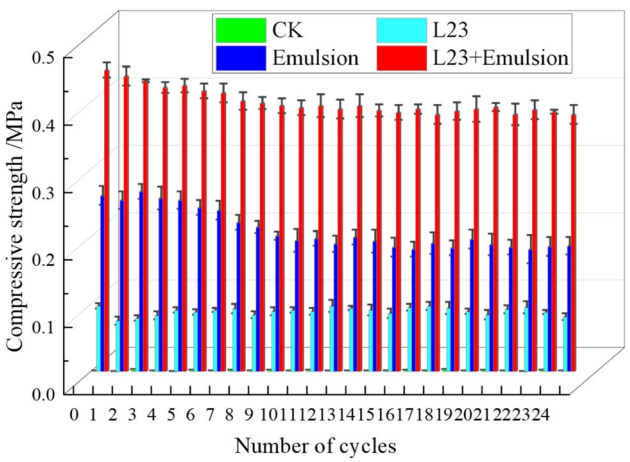

Fig. 14 Variations in compressive strength of stabilized sand specimens with thermal cycling frequency.

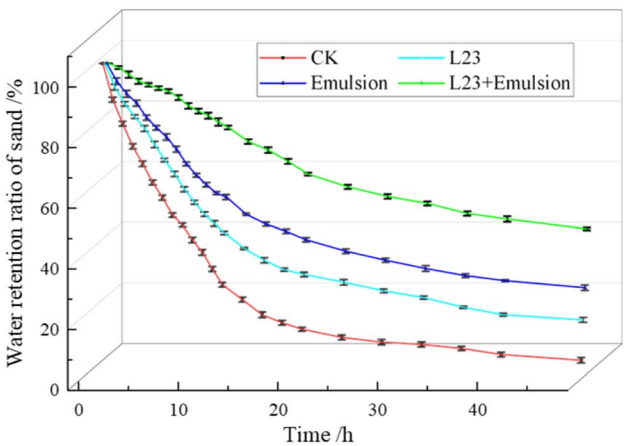

Fig. 16 The relationship between L23 content and the water content of sand with 3.0 wt% NaCl at different evaporating time under 298 K.

© 2025 The Author(s). Published by the Royal Society of Chemistry

Open Access Article. Published on 08 December 2025. Downloaded on 2/15/2026 4:40:46 PM. This article is licensed under a Creative Commons Attribution-NonCommercial 3.0 Unported Licence.

performance of the material was significantly improved after adding L23.

Moreover, within the same time frame, the water retention capacity of the samples increased with higher concentrations of L23 in the emulsion. This could be attributed to the addition of L23, which reduced the surface tension between the emulsion and sand particles, thereby enhancing the spreading and film-forming properties of the emulsion at the interface and improving its durability. According to the single molecular insoluble film theory, water evaporation was the process by which H_2O molecules of water surface changes from a liquid to a gas or vapour. When water molecules escape from the surface, the resulting molecular film generates an interfacial force that suppresses evaporation. Increasing the amount of L23 promoted the formation of a denser crust on the sand surface, thereby enhancing moisture retention. In addition, while inhibiting water evaporation, L23 also effectively suppressed the upward movement of salt in the sand, reducing salt accumulation on the surface. This improvement contributed to the enhanced sand-fixing effectiveness of the material and supported the growth of plants and microorganisms in the sand.[78] In summary, the incorporation of L23 into the emulsion significantly reduced the water evaporation rate and improved water retention performance. This may be important for germination and growth in halophytes and reproduction of microbe in the salty desert, which would be planned in our future investigation.

3.7.7 Moisture of treated sand. Humidity is a key factor affecting microbial activity and plant growth in saline sandy soil. Fig. 17 illustrated that significant variations in moisture content were observed among the sand samples treated with different sand-fixing materials over the six-month testing period. Both L23 and emulsion treatments individually demonstrated positive effects on sand moisture content, with results significantly superior to the blank treatment. Furthermore, sand samples treated with the L23-emulsion composite material showed markedly higher humidity levels than those treated with emulsion alone, achieving a moisture increase exceeding 1.3 times. This indicated that the composite material could function as a "reservoir" in desert environments, storing water during rainfall and releasing it gradually, thereby providing a sustained water supply for the growth of psammophytic vegetation in highly saline sandy soils.

3.8 Ecological effect of L23 addition on sand fixation performance

3.8.1 Nutrient content of treated sand. In addition to water, nutrients are the other primary factor limiting plant growth. In wind-blown sand areas, the soil formation process is unstable due to wind erosion and sand burial, resulting in minimal organic matter accumulation and a lack of physical clay particles, which leads to fragile soil structure. Therefore, enhancing the accumulation of soil organic carbon and nutrient content can promote the restoration of degraded saline sandy soils.[79,80] Fig. 18(a–c) indicated that the L23+emulsion composite material increased the organic carbon content of treated sandy soil by at least 114.2%, the total nitrogen content by at least 13.1%, and the available potassium content by at least 22.7% compared to treatment with emulsion alone. This demonstrated that L23, by controlling salt crystal size and reducing phase separation, enhanced the density of the emulsion film formation, creating a stable three-dimensional network structure that effectively inhibited water evaporation and salt migration upward, thereby fostering favorable conditions for organic matter accumulation. Simultaneously, the microenvironment formed by the combination of its hydrophilic ended with moisture in the sandy soil adsorbs and slowly releases nutrients, promoting microbial activity and nutrient

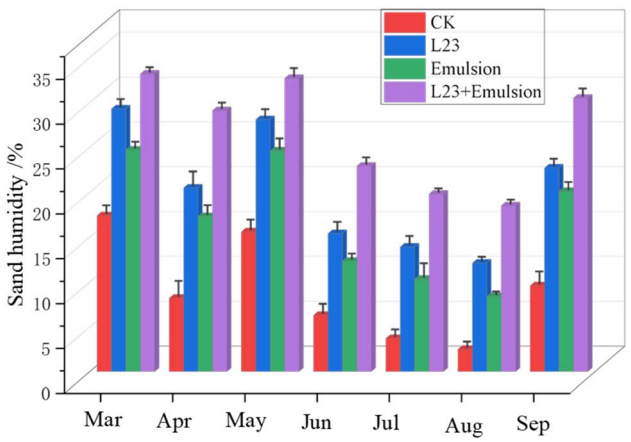

Fig. 17 Moisture of treated sand.

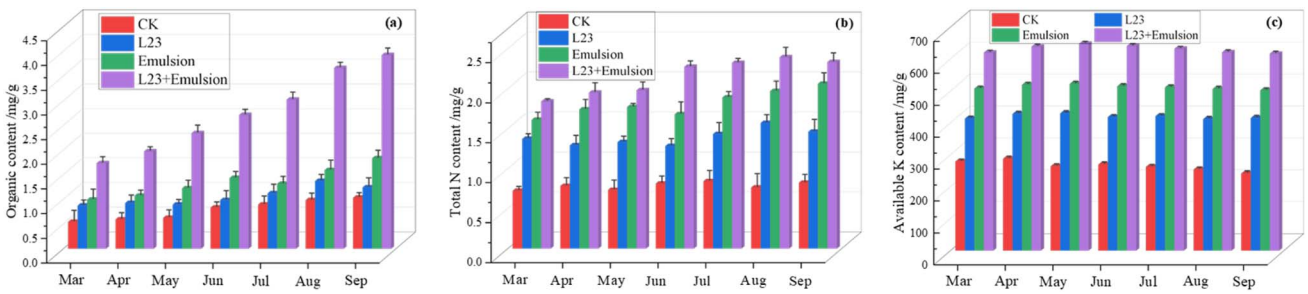

Fig. 18 Differences in physicochemical properties of the treated sand: (a) organic carbon contents, (b) total nitrogen contents, and (c) available potassium contents.

Open Access Article. Published on 08 December 2025. Downloaded on 2/15/2026 4:40:46 PM.
This article is licensed under a Creative Commons Attribution-NonCommercial 3.0 Unported Licence.

Fig. 19 Parallel images of the growth of tomato seedlings: (left) sand containing 3% NaCl with treatment of emulsion; (right) sand containing 3% NaCl treated by emulsion mixed L23.

transformation, thus significantly increasing the content and sustainable supply capacity of nutrients such as organic carbon, nitrogen, and potassium in the sandy soil. The changes in nutrient content in the sandy soil visually reflected that the combined use of L23 and emulsion has a significant impact on the transformation of sand into soil and the ecological restoration of vegetation.

3.8.2 Plant growth in treated sand. One of the most important considerations in ecological sand fixation is achieving vegetation restoration in sandy land. To study the effect of the L23 + emulsion composite sand-fixing material on plant growth, we conducted a planting experiment with tomato seedlings in sand containing 3% NaCl. The growth result of the tomato seedlings after 40 days were shown in Fig. 19. Compared to the use of emulsion alone, a clear difference in the growth of tomato seedlings was observed on the saline sand fixed with the L23 + emulsion composite material. The superior growth performance indicated the positive effect of the L23 + emulsion composite material on the restoration of saline sandy land. This growth disparity arised because the L23 + emulsion composite material could build bridges between moving sand particles, binding them together to form a sand-fixing layer with resistance to wind erosion, thereby providing a suitable and stable environment for plant growth. Furthermore, the addition of L23 significantly enhanced the water retention capacity of the sand-fixing material and increased the nutrient content in the sand, while reducing salt-induced osmotic pressure in the sandy soil, thus promoting the germination and growth of halophytes.

Accordingly, a field study has been implemented. Fig. 20 illustrated the growth performance of *Tall Fescue* on saline sand treated with the L23 + emulsion composite sand-fixing material under field conditions over a seven-month period from March to September. Compared to the application of emulsion alone, a distinct difference in plant growth was observed on the saline sand stabilized with the L23 + emulsion composite. *Tall Fescue* thrived in the sand treated with the L23 + emulsion material, exhibiting a seedling survival rate exceeding 60%, significantly higher than that in plots treated with emulsion only. Furthermore, stem biomass and plant height were markedly greater than those in the control group. The vigorous growth observed underscored the efficacy of the L23 + emulsion composite in restoring high-salinity sandy lands. Nevertheless, our primary long-term goal remains to achieve sustainable vegetation survival and flourishing within stabilized saline desert ecosystems. Further research is needed and should be related to both materials and *Tall Fescue*.

3.8.3 Microbial dynamics in treated sand. The microbial growth in saline sand treated with L23 + emulsion composite sand-fixing material was analyzed using the plate counting method, and the experimental results were shown in Fig. 21. The plate count data revealed that the quantities of both fungi and bact eria were noticeably lower than those of actinomycetes in all groups, including the control. This was likely due to the high salt concentration and nutrient-poor conditions in the sandy soil, which greatly restrict the proliferation of bacteria and fungi, resulting in noticeably lower counts compared to

Fig. 20 Parallel images of growth of *Tall Fescue* in field conditions: (left) treated by emulsion; (right) treated by emulsion mixed L23.

© 2025 The Author(s). Published by the Royal Society of Chemistry

Open Access Article. Published on 08 December 2025. Downloaded on 2/15/2026 4:40:46 PM.
This article is licensed under a Creative Commons Attribution-NonCommercial 3.0 Unported Licence.

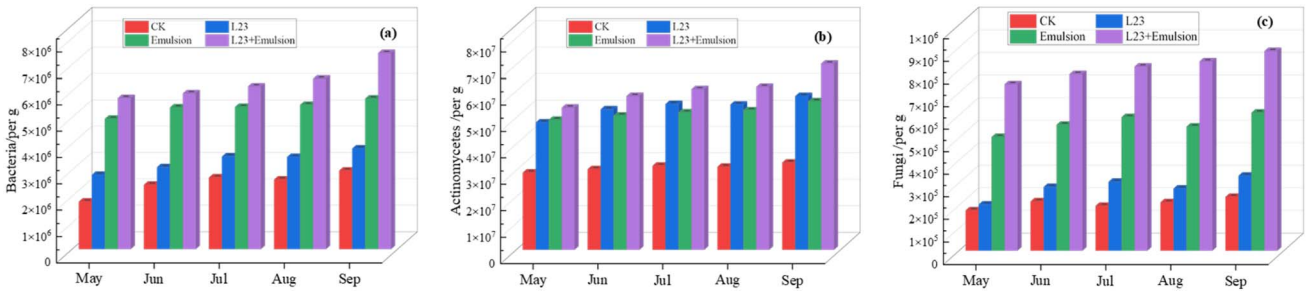

Fig. 21 Number of microbes of the treated sand: (a) bacteria, (b) actinomycetes, and (c) fungi.

actinomycetes. In contrast, the microbial population in the soil treated with the L23 + emulsion composite material showed a substantial increase compared to that treated with emulsion alone, demonstrating the favorable ecological effects of the L23 + emulsion composite. This improvement could be attributed to L23's ability to optimize the film-forming structure of the emulsion, creating a stable three-dimensional network that provided suitable habitats for microorganisms. Additionally, the hydrophilic ends of L23 formed a micro-environment by interacting with water, effectively reducing salinity stress in the soil solution, while the organic matter and nutrients released gradually from the composite film served as a sustained energy source for microbial metabolism. Together, these mechanisms significantly enhanced microbial colonization and reproduction. These findings indicated that the application of the L23 + emulsion composite sand-fixing material in saline desert remediation could meet the requirements for ecological restoration.

4 Conclusion

This study developed an L23 + emulsion composite eco-sand-fixing material to address salt crystallization damage in highly saline sandy lands. The results demonstrated that surfactant L23 significantly enhanced its adsorption capacity on sand particles through synergistic effects including double-layer compression and salting-out, effectively controlling NaCl crystallization morphology and inhibiting salt-induced damage. When compounded with P(VAc-DBM-AA-AM-IA-HBP) hyperbranched emulsion, the material exhibited comprehensively improved sand-fixing properties, including mechanical strength, wind erosion resistance, thermal aging resistance, and freeze–thaw stability, enabling it to withstand harsh desert conditions. Field experiments further confirmed that the material promoted plant and microbial growth, demonstrating good ecological compatibility. This research will provide a promising material design and technological pathway for desertification control in saline desert areas.

Author contributions

Conceptualization, Meilan Li; methodology and writing – original draft preparation, Wei Gong; data curation, Haonan Ji; formal analysis, Siying Liu; investigation, Shitong Xie; validation, Liangliang Chang. All the authors have read and agreed to the published version of the manuscript. All authors have read and agreed to the published version of the manuscript.

Conflicts of interest

The authors declare no conflicts of interest.

Data availability

The data used to support the findings of this study are available from the corresponding author upon request due to privacy reasons.

Acknowledgements

This work was financially supported by the Natural Science Basic Research Program of Shaanxi (Program No. 2023-JC-YB-108), the Natural Science Basic Research Program of Shaanxi (Program No. 2025SF-YBXM-272), and the Natural Science Basic Research Program of Shaanxi (Program No. 2025SYS-SYSZD-057); Shaanxi Province Youth Innovation Team Research Project (No. 24JP052).

References

1 T. J. Ren, L. M. Yuan, Y. Gao, *et al.*, Development and optimization of a plant-based sand fixer: Locust bean gum and its advanced materials, *Int. J. Biol. Macromol.*, 2025, **309**, 142514–142519.
2 X. Liang, P. Li, J. Wang, *et al.*, Research progress of desertification and its prevention in Mongolia, *Sustainability*, 2021, **13**, 6861–6869.
3 X. Tong, H. Yang, Z. Ning, *et al.*, Biomass estimation models for dominant sand-fixing shrubs in Horqin Sand Land, *J. Desert Res.*, 2018, **28**(3), 553–559.
4 J. K. Yuan, C. W. Ye, L. Luo, *et al.*, Sand fixation property and erosion control through new cellulose-based curing agent on sandy slopes under rainfall, *Bull. Eng. Geol. Environ.*, 2020, **79**, 4051–4061.
5 H. Zhao, X. Zhai, S. Li, *et al.*, The continuing decrease of sandy desert and sandy land in northern China in the latest 10 years, *Ecol. Indic.*, 2023, **154**, 110699–110705.

© 2025 The Author(s). Published by the Royal Society of Chemistry

Open Access Article. Published on 08 December 2025. Downloaded on 2/15/2026 4:40:46 PM. This article is licensed under a Creative Commons Attribution-NonCommercial 3.0 Unported Licence.

6 T. Wang, Land use and sandy desertification in the north China, *Desert Res.*, 2000, **20**, 103–113.
7 S. L. Liu, T. Wang, X. Song, *et al.*, Aeolian Desertification Monitoring in the Sandy Areas of Northern China[M], *Sandy Soils*, Springer Nature Switzerland, Cham, 2024, pp.101–112.
8 G. Singh, Salinity-related desertification and management strategies: Indian experience, *Land Degrad. Dev.*, 2009, **20**(4), 367–385.
9 X. Wang, X. Li, D. Cai, *et al.*, Salinification and salt transports under aeolian processes in potential desertification regions of China, *Sci. Total Environ.*, 2021, **782**, 146832–146839.
10 Y. Wang, Y. Zhao, L. Yan, *et al.*, Groundwater regulation for coordinated mitigation of salinization and desertification in arid areas, *Agric. Water Manag.*, 2022, **271**, 107758–107763.
11 X. Y. Meng, X. Gao, S. Li, *et al.*, Monitoring desertification in Mongolia based on Landsat images and Google Earth Engine from 1990 to 2020, *Ecol. Indic.*, 2021, **129**, 107908–107916.
12 Y. Liu, Q. Guo, L. M. Yuan, *et al.*, Effects of three plant-based sand-fixing agents on water infiltration and evaporation in aeolian sandy soil, *Arid Zone Res.*, 2025, **42**(4), 658–667.
13 Z. Dong, F. Xu and J. Yang, A novel approach to cost-effective utilization of flax polysaccharides: sand fixation, *Int. J. Biol. Macromol.*, 2025, **322**(3), 146925–146929.
14 X. Li, R. Zhou, H. Jiang, *et al.*, Quantitative analysis of how different checkerboard sand barrier materials influence soil properties: a study from the eastern edge of the Tengger Desert, China, *Environ. Earth Sci.*, 2018, **77**(13), 481–487.
15 Y. Yan, Q. Guan, W. Shao, *et al.*, Spatiotemporal dynamics and driving mechanism of arable ecosystem stability in arid and semi-arid areas based on Pressure-Buffer-Response process, *J. Cleaner Prod.*, 2023, **421**, 138553–138559.
16 B. Y. Xu, Y. H. Hou, Z. S. Yang, *et al.*, Management of saline-alkali sandy soils by amphoteric lignin-based sand fixation, *Int. J. Biol. Macromol.*, 2025, **311**(3), 144018–144024.
17 R. Yang, S. Chen, W. Zhao, *et al.*, Response of soil inorganic nitrogen dynamics to planting age and vegetation type in artificial sand-fixing land, *Ecosphere*, 2024, **15**(6), 4869–4873.
18 H. R. Ren, L. Tao, J. Ren, *et al.*, Chlorophyll and growth performance of biological sand-fixing materials inoculated on sandy desert surface, *Photosynthetica*, 2025, **62**(2), 213–218.
19 G. Wang, W. Zhao, H. Liu, *et al.*, Changes in soil and vegetation with stabilization of dunes in a desert-oasis ecotone, *Ecol. Res.*, 2015, **30**(4), 639–650.
20 Z. Zhang, Z. Li, L. Yao, *et al.*, Development and performance evaluation of sunflower straw cellulose ether ecological sand-fixing material, *BioResources*, 2024, **19**(2), 2201–2207.
21 T. J. Ren, L. M. Yuan, Y. Gao, *et al.*, Development and optimization of a plant-based sand fixer: Locust bean gum and its advanced materials, *Int. J. Biol. Macromol.*, 2025, **309**, 142514–142520.
22 Su Y. Alamusa, Q. Zhou, *et al.*, Artificial vegetation for sand stabilization may impact sand lake dynamics in dune regions, *Plants*, 2024, **13**(2), 255–261.
23 L. Zhong, X. Feng and W. Zhao, Fixing active sand dune by native grasses in the desert of Northwest China, *Ecol. Process.*, 2024, **13**(1), 77–83.
24 Y. W. Pei, L. M. Huang, M. A. Shao, *et al.*, Patterns and drivers of seasonal water sources for artificial sand-fixing plants in the northeastern Mu Us sandy land, Northwest China, *Pedosphere*, 2024, **34**(1), 63–77.
25 W. Gong, Y. X. Zang, B. L. Liu, *et al.*, Effect of using polymeric materials in ecological sand-fixing of Kerqin Sandy Land of China, *J. Appl. Polym. Sci.*, 2016, **133**(43), 44102–44109.
26 O. Alexandra, N. Elina, D. Emily, *et al.*, Synthesis of poly (isobutyl acrylate/n-butylacrylate/methyl methacrylate)/CNC nanocomposites for adhesive applications via in situ semi-batch emulsion polymerization, *Polym. Compos.*, 2019, **40**(4), 1365–1377.
27 Y. Li, P. Rao, J. Wang, *et al.*, Study on preparation and application of a multifunctional microspheric soil conditioner based on Arabic gum, gelatin, chitosan and β-cyclodextrin, *Int. J. Biol. Macromol.*, 2021, **183**, 1851–1860.
28 Z. H. Li, C. W. Chen, H. GaoY, *et al.*, Synergistic effect of cyanobacteria and nano-sand-stabilizer on biocrust formation and sand fixation, *J. Environ. Chem. Eng.*, 2021, **9**(1), 101–104.
29 W. Gong, M. L. Li, Y. X. Zang, *et al.*, The synthesis of salt-resistant emulsion and its application in ecological sand-fixing of high salt-affected sandy land, *Plast, Rubber Compos.*, 2017, **46**(4), 163–172.
30 J. K. Yuan, Z. Pei, S. L. Yang, *et al.*, Preparation and characterization of an eco-friendly sand-fixing agent utilizing nanosilica/polymer composites, *J. Appl. Polym. Sci.*, 2023, **140**(18), 53804–53817.
31 J. Yang, H. Cao, F. Wang, *et al.*, Application and appreciation of chemical sand fixing agent-poly (aspartic acid) and its composites, *Environ. Pollut.*, 2007, **150**(3), 381–384.
32 J. Wang, M. Liu, K. Han, *et al.*, Feasibility of agricultural utilization of river sludge as a planting substrate following treatment with polyacrylamide, *J. Cleaner Prod.*, 2022, **367**, 132964–132969.
33 Z. S. Liang, Z. R. Wu, M. Noori, *et al.*, Effect of simulated corrosion environment on mechanical performances of sand fixation by hydrophilic polyurethane, *Fresenius Environ. Bull.*, 2017, **26**, 5797–5805.
34 L. Chen, Y. Luo, J. Xu, *et al.*, Effects of different ratios of soft and rigid segment on the properties of soil and sand fixing materials of polyacrylate, *J. Polym. Eng.*, 2025, **45**(1), 42–49.
35 X. G. Dang, H. Chen and Z. H. Shan, Preparation and characterization of poly(acrylic acid)-corn starch blend for use as chemical sand-fixing materials, *Mater. Res. Express*, 2017, **4**, 075506–075510.
36 J. Liu, Q. Feng, Y. Wang, *et al.*, Experimental study on unconfined compressive strength of organic polymer reinforced sand, *Int. J. Polym. Sci.*, 2018, **12**, 1–18.
37 H. Xie, B. Liu, W. Wang, *et al.*, Ecological sand-fixing properties of polyurethane along comparison with

© 2025 The Author(s). Published by the Royal Society of Chemistry

Open Access Article. Published on 08 December 2025. Downloaded on 2/15/2026 4:40:46 PM. This article is licensed under a Creative Commons Attribution-NonCommercial 3.0 Unported Licence.

polyvinyl acetate emulsion, *Polym. Mater. Sci. Eng.*, 2018, **34**(3), 87–92.
38 L. Chen, Y. Luo, J. Xu, *et al.*, Effects of different ratios of soft and rigid segment on the properties of soil and sand fixing materials of polyacrylate, *J. Polym. Eng.*, 2025, **45**(1), 42–49.
39 W. Huang, X. Geng, Z. Liu, *et al.*, Molecular dynamics study of polymeric stabilizers as soil improvement materials, *Chem. Phys. Lett.*, 2022, **806**, 139985–139991.
40 W. Gao and Z. Wu, Study of Mechanism of the W-OH Sand Fixation, *J. Environ. Prot.*, 2012, **3**(9), 1025–1033.
41 W. S. Abdel-Wakil, T. M. Salama, E. A. Kamoun, *et al*, Waterborne nano-emulsions of polyvinyl acetate-polyurethane coatings containing different types of vinyl monomers: synthesis and characterization, *Pigm. Resin Technol.*, 2021, **52**(1), 7–18.
42 X. Meng, G. Peng, B. L. Liu, *et al.*, Synthesis and sand-fixing property of cationic poly(vinyl acetate-butyl acrylate-DMC) copolymer emulsions, *Polym.-Plast. Technol. Eng.*, 2013, **52**, 931–939.
43 X. Dang, H. Chen and Z. Shan, Preparation and characterization of poly(acrylic acid)-corn starch blend for use as chemical sand-fixing materials, *Mater. Res. Express*, 2017, **4**(7), 075506–075511.
44 T. Bal and S. Swain, Microwave assisted synthesis of polyacrylamide grafted polymeric blend of fenugreek seed mucilage-Polyvinyl alcohol (FSM-PVA-g-PAM) and its characterizations as tissue engineered scaffold and as a drug delivery device, *J. Pharmaceut. Sci.*, 2020, **28**, 33–44.
45 H. Yang, M. Liu, N. Wang, *et al.*, Preparation and water erosion resistance properties of Tara gum-G-poly (acrylic acid-co-methyl methacrylate) emulsion, *Int. J. Biol. Macromol.*, 2023, **242**, 124645–124651.
46 W. Gong, M. . L. Li, B. L. Liu, *et al.*, An amphoteric poly(VAc-DBM-AM-DMAPS) emulsion focusing on the ecological sand-fixing in salty desert: Structure and properties, *J. Appl. Polym. Sci.*, 2016, **133**(30), 43715–43726.
47 W. Gong, M. L. Li, B. L. Liu, *et al.*, How the surfactants mixed with emulsion can enhance the sand fixation ability in the high salt-affected sandy land, *Environ. Technol.*, 2021, **42**(16), 2516–2526.
48 M. J. Scott and M. N. Jones, The biodegradation of surfactants in the environment, *Biochim. Biophys. Acta Biomembr.*, 2000, **1508**(1–2), 235–251.
49 A. Franzetti, P. Di Gennaro, A. Bevilacqua, *et al.*, Environmental features of two commercial surfactants widely used in soil remediation, *Chemosphere*, 2006, **62**(9), 1474–1480.
50 S. D. Haigh, A review of the interaction of surfactants with organic contaminants in soil, *Sci. Total Environ.*, 1996, **185**(1–3), 161–170.
51 E. Olkowska, Z. Polkowska and J. Namiesnik, Analytics of surfactants in the environment: problems and challenges, *Chem. Rev.*, 2011, **111**(9), 5667–5700.
52 G. G. Ying, Fate, behavior and effects of surfactants and their degradation products in the environment, *Environ. Int.*, 2006, **32**(3), 417–431.
53 S. O. Badmus, H. K. Amusa, T. A. Oyehan, *et al.*, Environmental risks and toxicity of surfactants: overview of analysis, assessment, and remediation techniques, *Environ. Sci. Pollut. Res.*, 2021, **28**(44), 62085–62104.
54 Y. Q. Wang, H. Cao, X. Y. Wang, *et al.*, Experimental and theoretical investigation on the mechanism of cationic surfactants-assisted phosphogypsum crystal transformation, *Surf. Interfaces*, 2024, **47**, 104211–104218.
55 M. L. Li, Y. Y. Jin, J. L. Wan, *et al.*, Effectiveness of Applying Hyperbranched PVAc Copolymer Emulsion for Ecological Sand-Fixing in the High Salt-Affected Sandy Land, *Polymers*, 2025, **17**, 2403–2414.
56 S. Zhao, G. Tian, C. Zhao, *et al.*, The stability of three different citrus oil-in-water emulsions fabricated by spontaneous emulsification, *Food chem.*, 2018, **269**, 577–587.
57 A. Singh, K. A. Raj, A. M. MS, *et al.*, Investigation on rheological characterization and salt tolerance potential of paraffinic O/W emulsions of natural surfactant for crude emulsification and mobilization, *Ind. Eng. Chem. Res.*, 2024, **63**(24), 10825–10841.
58 A. K. Mathur, C. B. Majumder and S. Chatterjee, Combined removal of BTEX in air stream by using mixture of sugar cane bagasse, compost and GAC as biofilter media, *J. Hazard. Mater.*, 2007, **148**(1–2), 64–74.
59 T. M. S. Lima, L. C. Procópio, F. D. Brandão, *et al.*, Evaluation of bacterial surfactant toxicity towards petroleum degrading microorganisms, *Bioresour. Technol.*, 2011, **102**(3), 2957–2964.
60 Q. Zhou, B. T. Qin, B. H. Zhou, *et al.*, Effects of surfactant adsorption on the surface functional group contents and polymerization properties of coal dust, *Process Saf. Environ. Prot.*, 2023, **173**, 693–701.
61 X. Meng, L. Liang and B. Liu, Synthesis and sand-fixing properties of cationic poly (vinyl acetate-butyl acrylate-2-hydroxyethyl acrylate-DMC) copolymer emulsions, *J. Polym. Environ.*, 2017, **25**(2), 487–498.
62 Y. Zang, W. Gong, H. Xie, *et al.*, Evaluation and mechanism of anionic waterborne polyurethane dispersion for chemical sand stabilisation, *Plast., Rubber Compos.*, 2016, **45**(6), 270–276.
63 K. Goyal, N. Singh, S. Jindal, *et al.*, *Advanced Techniques Of Analytical Chemistry*, 2022, vol. 1(1), pp.105–109.
64 Q. Li, T. Li and J. Wu, Water solubilization capacity and conductance behaviors of AOT and NaDEHP systems in the presence of additives, *Colloids Surf. A*, 2002, **197**, 101–109.
65 W. Gong, Y. X. Zang, H. Xie, *et al.*, Properties of surfactants on high salt-affected sandy land in enhanced sand fixation: salt tolerance, adsorption isotherms and ecological effect, *RSC Adv.*, 2015, **5**(100), 81847–81856.
66 J. J. Sheng, Optimum phase type and optimum salinity profile in surfactant flooding, *J. Petrol. Sci. Eng.*, 2010, **75**, 143–153.
67 R. Lu, S. He, T. Wang, *et al.*, Low-cost preparation of temperature-resistant and salt-tolerant amphiphilic carbon dots from a nonionic surfactant and its application in enhanced oil recovery, *Carbon*, 2024, **225**, 119104–119110.

Open Access Article. Published on 08 December 2025. Downloaded on 2/15/2026 4:40:46 PM.
This article is licensed under a Creative Commons Attribution-NonCommercial 3.0 Unported Licence.

68 M. J. Qazi, R. W. Liefferink, S. J. Schlegel, *et al.*, Influence of surfactants on sodium chloride crystallization, *Langmuir*, 2017, **33**(17), 4260–4268.
69 M. S. Bakshi, How surfactants control crystal growth of nanomaterials, *Cryst. Growth Des.*, 2016, **16**(2), 1104–1133.
70 W. Huang, X. Geng, J. Li, *et al.*, Molecular dynamics study on the adsorption and modification mechanism of polymeric sand-fixing agent, *Polymers*, 2022, **14**, 3365–3372.
71 J. K. Yuan, X. J. Pei, C. W. Ye, *et al.*, Experiments on adsorption mechanics and disintegration characteristics of modified cellulose-based polymer sand fixers, *J. Agric. Eng.*, 2019, **35**(21), 144–150.
72 A. W. Marczewski, Analysis of kinetic Langmuir model. Part I: integrated kinetic Langmuir equation (IKL): a new complete analytical solution of the Langmuir rate equation, *Langmuir*, 2010, **26**(19), 15229–15238.
73 W. J. Yang and B. L. Liu, Degradable cellulose acetate-based waterborne polyurethane sand-fixing agents for sand control in desert regions, *Polym. Test.*, 2024, **137**, 108512–108522.
74 H. Wang, R. Zhao, X. Wu, *et al.*, Preparation and properties of bio-based attapulgite copolymer (BAC) sand-fixing material, *Polymers*, 2023, **15**(2), 265–277.
75 M. Suraj Belgaonkar and B. Kandasubramanian, Hyperbranched polymer-based nanocomposites: synthesis, progress, and applications, *Eur. Polym. J.*, 2021, **147**, 110301–110310.
76 Y. Ahmadi and K. H. Kim, Hyperbranched polymers as superior adsorbent for the treatment of dyes in water, *Adv. Colloid Interface Sci.*, 2022, **302**, 102633–102641.
77 Y. Jiang, H. Sun, S. Zhang, *et al.*, Water retention material performance tests and ecological rehabilitation strategies for water-scarce abandoned mining sites in Northwestern China, *Environ. Monit. Assess.*, 2025, **197**(4), 399.
78 Y. F. Tong, Y. Q. Liu, M. S. Gong, *et al.*, Using a simple coating strategy to evolve polylactic acid into sand-fixation material with nutrient-rich reservoir by strong H-bonding interaction at phase interface, *Appl. Surf. Sci.*, 2024, **650**, 159205–159210.
79 J. A. Pujol, J. F. Calvo and D. L. Ramirez, Recovery of germination from different osmotic conditions by four halophytes from southeastern Spain, *Ann. Bot.*, 2000, **85**(2), 279–286.
80 M. Gorai, W. Aloui, X. Yang, *et al.*, Toward understanding the ecological role of mucilage in seed germination of a desert shrub Henophyton deserti: interactive effects of temperature, salinity and osmotic stress, *Plant Soil*, 2014, **374**(1), 727–738.

© 2025 The Author(s). Published by the Royal Society of Chemistry